PARAMETRIZED MAXIMUM PRINCIPLE PRESERVING FLUX LIMITERS FOR HIGH ORDER SCHEMES SOLVING HYPERBOLIC CONSERVATION LAWS: ONE-DIMENSIONAL SCALAR PROBLEM

ZHENGFU XU

ABSTRACT. In this paper, we present a class of parametrized limiters used to achieve strict maximum principle for high order numerical schemes applied to hyperbolic conservation laws computation. By decoupling a sequence of parameters embedded in a group of explicit inequalities, the numerical fluxes are locally redefined in consistent and conservative formulation. We will show that the global maximum principle can be preserved while the high order accuracy of the underlying scheme being maintained. The parametrized limiters are less restrictive on the CFL number when applied to high order finite volume scheme. The less restrictive limiters allow for the development of the high order finite difference scheme which preserves the maximum principle. Within the proposed parametrized limiters framework, a successive sequence of limiters are designed to allow for significantly large CFL number by relaxing the limits on the intermediate values of the multi-stage Runge-Kutta method. Numerical results and preliminary analysis for linear and nonlinear scalar problems are presented to support the claim. The parametrized limiters are applied to the numerical fluxes directly. There is no increased complexity to apply the parametrized limiters to different kinds of monotone numerical fluxes.

1. INTRODUCTION

Recently, Zhang & Shu [12] developed a class of maximum principle preserving (MPP) limiters applied to the reconstructed high order polynomials in the finite volume framework and the representing high order polynomials in the RK discontinuous Galerkin (RKDG) methods for scalar hyperbolic conservation laws

$$(1.1) \qquad u_t + \nabla \cdot \mathbf{F}(u) = 0, u(\mathbf{x}, 0) = u_0(\mathbf{x}).$$

The complication of solving nonlinear hyperbolic problems (1.1) arises from the fact that irregularity could be developed in a short time period even the initial data is smooth. It demands the consideration of the physically relevant weak solution, so-called entropy solution to select a unique weak solution [4]. An important property of the entropy solution is that it preserves the strict maximum principle, namely

$$(1.2) \qquad u_m \le u(x, y, t) \le u_M \quad \text{if} \quad u_m \le u_0(x, y) \le u_M.$$

An example at the discrete level is the total variation diminishing (TVD) schemes by Harten [1] satisfying the strict maximum principle. However, it is well known

that the TVD scheme, where the total variation is measured by that of grid values, degenerates to first order accuracy at extrema [5]. In the high order formulation of one dimensional scalar problem

(1.3) $u_t + f(u)_x = 0, u(x, 0) = u_0(x),$

semi-discrete high order finite volume schemes [14, 7, 3] with TVD property were proposed. While the schemes satisfy the strict maximum principle and even local maximum principle [3], the time evolution is implemented by characteristic method, therefore only feasible in one dimension. It was not until the recent work [12], a genuinely high order conservative scheme was designed to preserve the global maximum principle. The technique was later generalized to positivity preserving (of density and pressure) high order discontinuous Galerkin (DG) or finite volume schemes for compressible Euler equations [13]. The MPP schemes are designed based on the observation that not only the average volume of an underlying function but also the function value itself should be bounded by the maximum and minimum values of the function. The simple observation was held true for the reconstructed polynomial after applying the MPP limiters, in the sense of rescaling the reconstructed polynomial when necessary without destroying the designed accuracy of the high order reconstruction. The innovative schemes designed by the authors maintain high order accuracy while preserving the global maximum principle. Here we refer to [12, 13] for the details.

In this paper, we would like to provide a different perspective regarding how to achieve the MPP while preserving high order accuracy by applying limiting parameters to the numerical flux. Thereby, the major difference between this approach and the work in [12] is that the focus here is on the numerical flux only. The reconstruction can be any strategy in the literature, e.g., adaptive, hierarchy or central high order reconstruction. The limiters can also be applied to numerical fluxes with high order polynomial representation of the solution like in the Runge-Kutta DG scheme. Another major difference is that our approach as presented through the main algorithm in Section 4.3 allows for significantly large CFL number. The large CFL number is achieved by relaxing the limits on the intermediate values for multi-stage TVD Runge-Kutta (RK) time discretization.

To illustrate the idea of parametrized limiters, we can start with the problem (1.3) on the interval $[0, T] \times [0, 1]$ with unspecified initial condition and periodic boundary. Let k be the time step size, $x_j = (j - \frac{1}{2})h$ and $x_{j+\frac{1}{2}} = jh$, $j = 0, 1, ...N$ for a uniform partition $h = 1/N$. Cell I_j is defined by the interval $[x_{j-\frac{1}{2}}, x_{j+\frac{1}{2}}]$. Without distinguishing point value and cell average evolution, we will choose u_j^n as approximate value produced by the one step forward Euler scheme

(1.4) $u_j^{n+1} = u_j^n - \lambda(\hat{H}_{j+\frac{1}{2}} - \hat{H}_{j-\frac{1}{2}}),$

where $\lambda = \frac{k}{h}$ is the CFL number. u_j^n could be approximate value of the solution $u(x_j, t_n)$ or its average $\frac{1}{h} \int_{x_{j-\frac{1}{2}}}^{x_{j+\frac{1}{2}}} u(x, t_n)dx$. After all, the conservative finite difference and finite volume methods for solving (1.3) take the similar form as in (1.4). $\hat{H}_{j+\frac{1}{2}}$ is the high order numerical flux, the numerical approximation of the local Riemann solver for the high order finite volume scheme. Let $u_m = \min_x(u(x, 0))$ and $u_M = \max_x(u(x, 0))$. Assuming the property that needs to be satisfied is that

$$u_m \leq u_j^n \leq u_M$$

and the current numerical fluxes $\hat{H}_{j+\frac{1}{2}}$ may not be able to guarantee such property, we resort to the limiters of the type

(1.5)
$$\tilde{H}_{j+\frac{1}{2}} = \theta_{j+\frac{1}{2}}(\hat{H}_{j+\frac{1}{2}} - \hat{h}_{j+\frac{1}{2}}) + \hat{h}_{j+\frac{1}{2}}$$

such that

(1.6)
$$u_m \leq u_j^n - \lambda(\tilde{H}_{j+\frac{1}{2}} - \tilde{H}_{j-\frac{1}{2}}) \leq u_M.$$

Here $\hat{h}_{j+\frac{1}{2}}$ is a first order monotone numerical flux that preserves the strict maximum principle

(1.7)
$$u_m \leq u_j^n - \lambda(\hat{h}_{j+\frac{1}{2}} - \hat{h}_{j-\frac{1}{2}}) \leq u_M.$$

Therefore, the problem becomes whether there are locally defined $\theta_{j+\frac{1}{2}}$'s satisfying (1.6). Meanwhile, for the purpose of high order accuracy, we would like the change of the numerical flux $\tilde{H}_{j+\frac{1}{2}} - \hat{H}_{j+\frac{1}{2}}$ after applying limiters stays on the scale of the desired truncation error of the underlying scheme.

However, in the sequence of inequalities (1.6), the parameters $\theta_{j+\frac{1}{2}}$'s are coupled together. In order to define the numerical flux in a local, conservative fashion, we need to find explicit constraint on each of the $\theta_{j+\frac{1}{2}}$'s. Before we continue to discuss the decoupling of (1.6), we would like to make the following comments:

Remark 1. *The MPP finite volume or discontinuous Galerkin limiters can be* **parametrized** *in the sense, that there are a group of locally defined values $\Lambda_{j+\frac{1}{2}}$'s such that for any sequence of $\theta_{j+\frac{1}{2}}$, if $\theta_{j+\frac{1}{2}} \in [0, \Lambda_{j+\frac{1}{2}}]$ for $j = 0, 1, 2, ...N$, then MPP is maintained. The limiting process introduced in [12] is consistent with this description when applied to linear problem.*

Remark 2. *$\theta_{j+\frac{1}{2}} = 0$ for $j = 0, 1, 2, ...N$ corresponds to the first order MPP approximation. $\theta_{j+\frac{1}{2}} = 1$ for $j = 0, 1, 2, ...N$ corresponds to the high order approximation without limiters. Therefore most of the the numerical fluxes we have seen so far are limited toward the first order monotone flux, especially the limiters used for various stability consideration.*

The numerical flux limiters designed for preserving particular solution structure do not fall into this category. As an example, the anti-diffusive flux we designed in [11] is not limited toward the first order monotone flux.

The original work by Zhang & Shu [12] can also be interpreted in the framework of coupled inequalities. The decoupling of (1.6) was carried out with the recognition that $u_m \leq u(x_\alpha) \leq u_M$ (x_α represents Gauss Lobatto quadrature points) when solving (1.3) by finite volume schemes or DG method. The original idea and the limiting process was constructive and intuitively straightforward. The difference is that the problem was addressed at the reconstruction level in [12], however, at the level of building the numerical flux right after reconstruction in our approach. The motivation of this work comes from the fact that there is tremendous difficulty to generalize the idea in [12] to the high order finite difference method since the maximal and minimal values for $H_{j+\frac{1}{2}}$ are partition dependent. Here the sliding function H was introduced by Osher & Shu in [9] satisfying

(1.8)
$$f(u(x)) = \frac{1}{h} \int_{x-\frac{h}{2}}^{x+\frac{h}{2}} H(\xi)d\xi.$$

It is very difficult if not completely impossible to rescale the reconstructed polyno-mial for $H(x)$ to achieve MPP without destroying the high order accuracy. Within the proposed flux limiting framework, a genuinely high order finite difference MPP scheme is presented in Section 4. We also want to point out that the high order finite difference MPP scheme presented in this paper is different from the positivity preserving finite difference scheme designed recently by Zhang & Shu [15] for com-pressible Euler equation. In [15], the design of the limiters relies on the assumption that the exact density is genuinely larger than a positive constant. Strictly speak-ing, the scheme described in [15] is not high order finite difference MPP scheme. There is no such requirement for the high order finite difference MPP scheme that we will discuss later in the paper.

Another observation of the Zhang & Shu limiters is that the limiting process is based on one step Euler forward time stepping. Each of the intermediate values is enforced to be within the range of $[u_m, u_M]$. For the TVD RK method, since u_j^{n+1} is a convex combination of intermediate values, this provides a sufficient condition for u_j^{n+1} to be within the range $[u_m, u_M]$. However, the accuracy inconsistency between the first order time-stepping and the high order space discretization when implementing the MPP idea inevitably leads to constraint on the CFL number (the time step size) as has been observed but not addressed in [12]. Consider that the intermediate values are not high order approximation of any numbers of interest, it is reasonable to relax the requirement on the intermediate values in a controlled manner and only enforce the final values be within the bounds. This new perspec-tive leads to the designing of high order finite volume and finite difference schemes with successive parametrized flux limiters which preserve maximum principle and high order accuracy without restrictive CFL constraint.

The rest of the paper is organized as follows. In Section 2, the decoupling of (1.6) will be presented within the high order, conservative formulation. In Section 3, we shall discuss how the high order accuracy can still be maintained while the limiters are applied to a high order finite volume scheme with suitable CFL condition. In Section 4, we will show that for the Euler forward based approach in a multi-stage RK method, when the CFL number is small enough, namely $k = ch^{1.5}, c > 0$, the limiters applied to third order finite difference scheme maintain MPP and third order accuracy. Explanation is given as for why a constraint on CFL is necessary in the finite difference framework. In the same section, a successive flux limiting process for TVD RK method is proposed as the main algorithm. Numerical examples are given in both finite volume and finite difference framework for linear and nonlinear one-dimensional scalar problems. Conclusion will be made in Section 5.

2. Decoupling for MPP flux limiting parameters

In this section, we will discuss the decoupling of (1.6) to identify the parameters $\theta_{j+\frac{1}{2}}$'s which provide a sufficient condition for the conservative scheme to preserve maximum principle. This decoupling process will be used as the building block of the main algorithm presented in Section 4.3.

In the following discussion, without ambiguity, we will use u_j for u_j^n. The de-coupling of (1.6) is purely algebraic and straightforward. The basic idea is that, in order to obtain an independent pair of $(\theta_{j-\frac{1}{2}}, \theta_{j+\frac{1}{2}})$ on cell I_j for the numerical flux to be locally defined (the scheme to be conservative), we need to find a pair
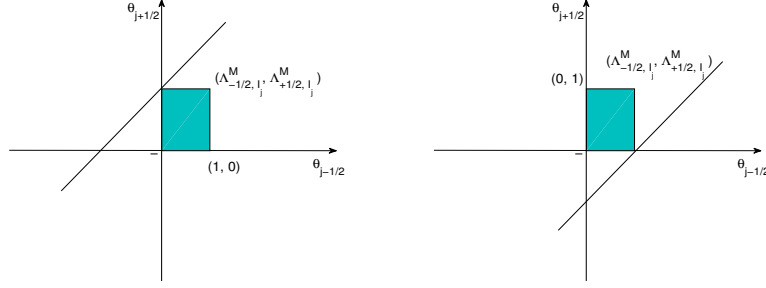
FIGURE 1. Decoupling (2.1): Case 2 and 3.

$(\Lambda_{-\frac{1}{2}, I_j}, \Lambda_{+\frac{1}{2}, I_j})$ such that any pair $(\theta_{j-\frac{1}{2}}, \theta_{j+\frac{1}{2}}) \in [0, \Lambda_{-\frac{1}{2}, I_j}] \times [0, \Lambda_{+\frac{1}{2}, I_j}]$ satisfies (1.6). For this purpose, we can rewrite the inequality (1.6) as

$$(2.1) \qquad \lambda \theta_{j-\frac{1}{2}}(\hat{H}_{j-\frac{1}{2}} - \hat{h}_{j-\frac{1}{2}}) - \lambda \theta_{j+\frac{1}{2}}(\hat{H}_{j+\frac{1}{2}} - \hat{h}_{j+\frac{1}{2}}) - \Gamma_j^M \leq 0,$$

where $\Gamma_j^M = u_M - u_j + \lambda(\hat{h}_{j+\frac{1}{2}} - \hat{h}_{j-\frac{1}{2}}) \geq 0$. For the minimum value part, we would like to have

$$(2.2) \qquad 0 \leq \lambda \theta_{j-\frac{1}{2}}(\hat{H}_{j-\frac{1}{2}} - \hat{h}_{j-\frac{1}{2}}) - \lambda \theta_{j+\frac{1}{2}}(\hat{H}_{j+\frac{1}{2}} - \hat{h}_{j+\frac{1}{2}}) - \Gamma_j^m,$$

where $\Gamma_j^m = u_m - u_j + \lambda(\hat{h}_{j+\frac{1}{2}} - \hat{h}_{j-\frac{1}{2}}) \leq 0$. For abbreviation, we could use the notation $F_{j+\frac{1}{2}} = \hat{H}_{j+\frac{1}{2}} - \hat{h}_{j+\frac{1}{2}}$. First, let us discuss the decoupling of (2.1) on cell I_j:

(1) If $F_{j-\frac{1}{2}} \leq 0$ and $F_{j+\frac{1}{2}} \geq 0$, it is obvious that the pair would be

$$(\Lambda_{-\frac{1}{2}, I_j}^M, \Lambda_{+\frac{1}{2}, I_j}^M) = (1, 1).$$

(2) If $F_{j-\frac{1}{2}} \leq 0$ and $F_{j+\frac{1}{2}} < 0$, the pair can be given as

$$(\Lambda_{-\frac{1}{2}, I_j}^M, \Lambda_{+\frac{1}{2}, I_j}^M) = (1, \min(1, \frac{\Gamma_j^M}{-\lambda F_{j+\frac{1}{2}}})).$$

(3) If $F_{j-\frac{1}{2}} > 0$ and $F_{j+\frac{1}{2}} \geq 0$, the pair can be given as

$$(\Lambda_{-\frac{1}{2}, I_j}^M, \Lambda_{+\frac{1}{2}, I_j}^M) = (\min(1, \frac{\Gamma_j^M}{\lambda F_{j-\frac{1}{2}}}), 1).$$

(4) If $F_{j-\frac{1}{2}} > 0$ and $F_{j+\frac{1}{2}} < 0$, when $(\theta_{j-\frac{1}{2}}, \theta_{j-\frac{1}{2}}) = (1, 1)$ satisfies (2.1), the pair can be given as $(\Lambda_{-\frac{1}{2}, I_j}, \Lambda_{+\frac{1}{2}, I_j}) = (1, 1)$. However, in the case that the pair $(\theta_{j-\frac{1}{2}}, \theta_{j-\frac{1}{2}}) = (1, 1)$ does not satisfy (2.1), intersection is given as the pair

$$(\Lambda_{-\frac{1}{2}, I_j}^M, \Lambda_{+\frac{1}{2}, I_j}^M) = (\frac{\Gamma_j^M}{\lambda F_{j-\frac{1}{2}} - \lambda F_{j+\frac{1}{2}}}, \frac{\Gamma_j^M}{\lambda F_{j-\frac{1}{2}} - \lambda F_{j+\frac{1}{2}}}).$$

The straight line in the figures is where

$$\lambda \theta_{j-\frac{1}{2}}(\hat{H}_{j-\frac{1}{2}} - \hat{h}_{j-\frac{1}{2}}) - \lambda \theta_{j+\frac{1}{2}}(\hat{H}_{j+\frac{1}{2}} - \hat{h}_{j+\frac{1}{2}}) - \Gamma_j^M = 0.$$
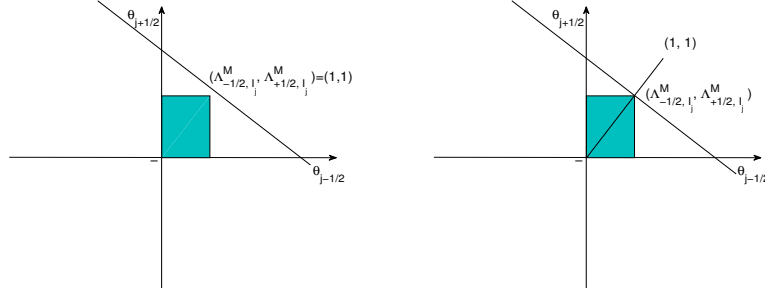
FIGURE 2. Decoupling (2.1): Case 4.

The negative sign at the origin indicates that the inequality (2.1) holds for the pair $(\theta_{j-\frac{1}{2}}, \theta_{j+\frac{1}{2}}) = (0,0)$. In the case of decoupling (2.2), the parameters can also be given symmetrically by

(1) If $F_{j-\frac{1}{2}} \geq 0$ and $F_{j+\frac{1}{2}} \leq 0$, the pair would be

$$(\Lambda^m_{-\frac{1}{2}, I_j}, \Lambda^m_{+\frac{1}{2}, I_j}) = (1, 1).$$

(2) If $F_{j-\frac{1}{2}} \geq 0$ and $F_{j+\frac{1}{2}} > 0$, the pair can be given as

$$(\Lambda^m_{-\frac{1}{2}, I_j}, \Lambda^m_{+\frac{1}{2}, I_j}) = (1, \min(1, \frac{\Gamma^m_j}{-\lambda F_{j+\frac{1}{2}}})).$$

(3) If $F_{j-\frac{1}{2}} < 0$ and $F_{j+\frac{1}{2}} \leq 0$, the pair can be given as

$$(\Lambda^m_{-\frac{1}{2}, I_j}, \Lambda^m_{+\frac{1}{2}, I_j}) = (\min(1, \frac{\Gamma^m_j}{\lambda F_{j-\frac{1}{2}}}), 1).$$

(4) If $F_{j-\frac{1}{2}} < 0$ and $F_{j+\frac{1}{2}} > 0$, when $(\theta_{j-\frac{1}{2}}, \theta_{j+\frac{1}{2}}) = (1, 1)$ satisfies (2.2), the pair can be given as $(\Lambda^m_{-\frac{1}{2}, I_j}, \Lambda^m_{+\frac{1}{2}, I_j}) = (1, 1)$. Again, in the case that $(\theta_{j-\frac{1}{2}}, \theta_{j+\frac{1}{2}}) = (1, 1)$ does not satisfy (2.2), intersection is given as the pair

$$(\Lambda^m_{-\frac{1}{2}, I_j}, \Lambda^m_{+\frac{1}{2}, I_j}) = (\frac{\Gamma^m_j}{\lambda F_{j-\frac{1}{2}} - \lambda F_{j+\frac{1}{2}}}, \frac{\Gamma^m_j}{\lambda F_{j-\frac{1}{2}} - \lambda F_{j+\frac{1}{2}}}).$$

The locally defined limiting parameter can be chosen to be

(2.3) $$\Lambda_{+\frac{1}{2}, I_j} = \min(\Lambda^M_{+\frac{1}{2}, I_j}, \Lambda^m_{+\frac{1}{2}, I_j}).$$

For the scheme to be conservative, we shall define the local limiting parameter for (1.6) as

(2.4) $$\theta_{j+\frac{1}{2}} = \Lambda_{j+\frac{1}{2}} = \min(\Lambda_{+\frac{1}{2}, I_j}, \Lambda_{-\frac{1}{2}, I_{j+1}}).$$

Therefore, the modified MPP numerical flux will be

(2.5) $$\tilde{H}_{j+\frac{1}{2}} = \theta_{j+\frac{1}{2}}(\hat{H}_{j+\frac{1}{2}} - \hat{h}_{j+\frac{1}{2}}) + \hat{h}_{j+\frac{1}{2}}.$$

The flux redefined by (2.5) is obviously consistent since it is a convex combination of high order flux with the first order flux. We would like to comment that

Remark 3. *For the scheme to achieve MPP property through the above procedure, the construction of the parametrized limiters does not rely on the high order polynomial reconstructing process, i.e., the ENO, WENO, or central WENO reconstruction. It only requires that the first order scheme to preserve maximum principle.*

Remark 4. *Since intuitively the limiters are only needed for cells close to global extrema, they will not take away the excellent capability of the regular ENO, WENO schemes for resolving shock, contact type interfacial structure. For locally MPP, or TVD type scheme, the limiters can be designed in the same way.*
By decoupling the inequalities (1.6) in the above manner, we shall state the first result

Theorem 5. *The scheme (1.4) for solving (1.3) with newly defined numerical flux (2.5) maintains the global maximum principle.*

The proof won't be necessary because of the way that the limiters are designed. So far, the limiters defined by (2.3) and (2.4) provide a sufficient condition for the underlying scheme to be MPP. A similar approach was investigated by Sweby [10] to explore the total variation diminishing (TVD) limiters for a class of Entropy-schemes for hyperbolic conservation laws. Since the scheme after the limiting process was enforced to be TVD, the scheme there was at most first order accurate in L^1. For the limiting process described above, the question remains whether the limiting procedure compromises the designed order of approximation and under what condition, it maintains the desired high order accuracy. These questions shall be answered in the following sections.

3. PARAMETRIZED LIMITERS FOR HIGH ORDER FINITE VOLUME SCHEME

In this section, advection equation and Burgers' equation are both computed using a third order finite volume ENO scheme and a third order finite volume with fixed stencil reconstruction with parametrized limiters to show the accuracy of the approximation. Results are also compared to the high order finite volume ENO scheme with Zhang & Shu limiters in [12]. The third order scheme is chosen as the example because of the consistency of order in space and time discretization when third order TVD RK time discretization is applied. Therefore, we can have a clear understanding of how the CFL number affects the performance of the scheme with parametrized flux limiters. Through the numerical tests within the finite volume framework, we would like to make the following points:

(1) The choice of CFL number affects the accuracy of the numerical approximation. In order to obtain the designed order of accuracy with the parametrized flux limiters, suitable CFL needs to be chosen.
(2) Preliminary analysis is given as explanation more than proof of why a mild constraint on the CFL is necessary. However, when the parametrized MPP flux limiters proposed in Section 2 are applied to each of the Euler forward steps in the TVD RK third order finite volume scheme, the CFL can be slightly larger than the CFL number proposed in [12]. This is confirmed both analytically and numerically.
(3) The MPP flux limiting technique does not depend on the reconstruction strategy for high order schemes.

3.1. **Computation of the advection equation.** First, we would like to check the order of accuracy if the finite volume scheme with parametrized limiters is used to solve the advection problem $f(u) = u$. On the interval $[0,1]$, we will compute the solution to the advection problem with initial condition $u(x,0) = \sin(2\pi x)$ assuming periodic boundary condition and $T = 1$. In space discretization, we choose third order finite volume reconstruction. The high order numerical flux $\hat{H}_{j+\frac{1}{2}}$ is the interface value $u_{j+\frac{1}{2}}^-$ reconstructed by the third order Harten ENO scheme [2] using average integral $\bar{u}_j$ over the cells I_j's while the first order flux is chosen as $\hat{h}_{j+\frac{1}{2}} = \bar{u}_j$. For the time stepping, we use the following third order TVD RK method to be consistent with space discretization accuracy. The third order TVD RK method for an ordinary differential equation $u_t = L(u)$ has the following form [8]:

$$
\begin{aligned}
u^{(1)} &= u^n + \Delta t L(u^n), \\
u^{(2)} &= \frac{3}{4}u^n + \frac{1}{4}u^{(1)} + \frac{1}{4}\Delta t L(u^{(1)}), \\
u^{n+1} &= \frac{1}{3}u^n + \frac{2}{3}u^{(2)} + \frac{2}{3}\Delta t L(u^{(2)}).
\end{aligned}
$$

It can also be written in the form of a combination of multiple Euler forward steps:

$$
\begin{aligned}
u^{(1)} &= u^n + \Delta t L(u^n), \\
(3.1) \quad u^{(2)} &= \frac{3}{4}u^n + \frac{1}{4}(u^{(1)} + \Delta t L(u^{(1)})), \\
u^{n+1} &= \frac{1}{3}u^n + \frac{2}{3}(u^{(2)} + \Delta t L(u^{(2)})).
\end{aligned}
$$

Therefore the Euler forward based limiting procedure described in Section 2 can be applied to each of the steps in (3.1) to ensure MPP property. In the work [12], as it is pointed out by the authors that in order for the finite volume scheme with polynomial of order 2 reconstruction to be MPP, the CFL number has to be less than $\frac{1}{6}$. However, for the method discussed in the last two sections, the construction of the limiters indicates that as long as CFL number is less than 1, the scheme with the parametrized limiters always maintain MPP. However, the order of accuracy will decrease while increasing CFL number. The choice of suitable CFL number is meant to ensure high order accuracy in this framework. In Table 1, we choose $CFL = 0.15, 0.2, 0.25$ separately using Harten's ENO scheme [2] to construct $u_{j+\frac{1}{2}}^-$ which is used as $\hat{H}_{j+\frac{1}{2}}$ in the limiting process described in Section 2. Comparing the

TABLE 1. Third order finite volume ENO scheme with parametrized limiters: advection equation.

	CFL=0.15		CFL=0.2		CFL=0.25	
N	L_∞ error	order	L_∞ error	order	L_∞ error	order
40	2.18E-3		2.04E-3		2.13E-3	
80	2.71E-4	3.00	2.56E-4	3.00	2.75E-4	2.95
160	3.37E-5	3.00	3.19E-5	3.00	4.15E-5	2.72
320	4.18E-6	3.01	3.99E-6	3.00	8.28E-6	2.32
640	5.18E-7	3.01	4.98E-7	3.00	2.07E-6	1.99

numerical result shown in Table 1 with the analysis in [12], with the parametrized limiters, the third order finite volume ENO scheme produces third order accurate approximation when CFL number is less than $1/5$ instead of $1/6$. This is attributed to the mild difference between those two approach that **in the parametrized limiting procedure, the limited end point value $u^-_{j+\frac{1}{2}}$ are not restricted to be in the range of $[u_m, u_M]$**, even though limiting the reconstructed values into the range of $[u_m, u_M]$ is a natural requirement in the finite volume framework. It seems that the requirement poses to be a stiff hurdle for designing high order MPP finite difference scheme. The new alternative approach introduced in the last two sections provides the opportunity of overcoming this hurdle.

3.2. **Computation of Burgers' equation.** In this part of the paper, we will present the numerical experiment of the flux limiting technique to the general non-linear problem (1.3). Through the numerical test, we would like to show:

(1) The parametrized limiting process for nonlinear problem preserves maximum principle without destroying the designed order of accuracy with suitable CFL number.
(2) The limiting process can be applied to different numerical flux other than upwinding flux without increased complexity.
(3) The CFL number can still be slightly larger than $1/6$ as suggested in [12] due to the fact that the reconstructed interface values $u_{j+\frac{1}{2}}$'s are not demanded to be in the range of $[u_m, u_M]$.

When the high order reconstruction is applied to recover the values $u^+_{j+\frac{1}{2}}$ and $u^-_{j+\frac{1}{2}}$ at interface, the high order flux $\hat{H}_{j+\frac{1}{2}}$ in the described limiting process takes the form

$$(3.2) \qquad \hat{H}_{j+/2} = F_{fl}(u^-_{j+\frac{1}{2}}, u^+_{j+\frac{1}{2}})$$

when Lax-Friedrich flux

$$(3.3) \qquad F_{fl}(a, b) = \frac{1}{2}(f(a) + f(b) - \alpha(b - a))$$

is used, where $\alpha = \max_u |f'(u)|$. It is obvious that when the first order numerical flux $\hat{h}_{j+/2} = F_{fl}(\bar{u}_j, \bar{u}_{j+1})$ is used, the scheme has MPP property. The redefined numerical flux has the following form

$$(3.4) \qquad \tilde{H}_{j+\frac{1}{2}} = \theta_{j+\frac{1}{2}}(\hat{H}_{j+\frac{1}{2}} - F_{fl}(\bar{u}_j, \bar{u}_{j+1})) + F_{fl}(\bar{u}_j, \bar{u}_{j+1}).$$

The corresponding sufficient condition for the high order scheme to be MPP can be written as

$$(3.5)\ \lambda\theta_{j-\frac{1}{2}}(\hat{H}_{j-\frac{1}{2}} - F_{fl}(\bar{u}_{j-1}, \bar{u}_j)) - \lambda\theta_{j+\frac{1}{2}}(\hat{H}_{j+\frac{1}{2}} - F_{fl}(\bar{u}_j, \bar{u}_{j+1})) - \Gamma^M_j \leq 0$$

for the maximum value part. Here

$$\Gamma^M_j = u_M - \bar{u}_j + \lambda F_{fl}(\bar{u}_j, \bar{u}_{j+1}) - \lambda F_{fl}(\bar{u}_{j-1}, \bar{u}_j) \geq 0.$$

For the minimum value part, it can be written as

$$(3.6)\ 0 \leq \lambda\theta_{j-\frac{1}{2}}(\hat{H}_{j-\frac{1}{2}} - F_{fl}(\bar{u}_{j-1}, \bar{u}_j)) - \lambda\theta_{j+\frac{1}{2}}(\hat{H}_{j+\frac{1}{2}} - F_{fl}(\bar{u}_j, \bar{u}_{j+1})) - \Gamma^m_j,$$

where $\Gamma^m_j = u_m - \bar{u}_j + \lambda F_{fl}(\bar{u}_j, \bar{u}_{j+1}) - \lambda F_{fl}(\bar{u}_{j-1}, \bar{u}_j) \leq 0$. The same decoupling process described in Section 2 can be applied.

In the case of inviscid Burgers' equation $f(u) = \frac{u^2}{2}$ with initial condition $u(x,0) = 0.5(1 + \sin(2\pi x))$ on the interval $[0,1]$, we run the simulation to $T = \frac{1}{2\pi}$ on a uniformly distributed partitions. Here we choose a fixed stencil, namely $S_j = \{I_{j-1}, I_j, I_{j+1}\}$ to reconstruct the values at interface, $u^-_{j+\frac{1}{2}}$ and $u^+_{j-\frac{1}{2}}$. The choice of fixed stencil is only to avoid the order degeneracy due to the frequent switching of stencils in the adaptive stencil-picking process of the Harten ENO scheme [6], which is not the issue we consider here. This is also an example that the reconstruction process is relatively irrelevant for preserving MPP property in the parametrized limiters framework. Third order RK method (3.1) is applied to the time discretization. In both linear and nonlinear cases, the error is measured by

TABLE 2. Third order finite volume scheme with parametrized limiters: Burgers' equation.

	CFL=0.15		CFL=0.2		CFL=0.4	
N	L_∞ error	order	L_∞ error	order	L_∞ error	order
40	1.90E-3		1.89E-3		1.87E-3	
80	2.80E-4	2.75	2.80E-4	2.75	2.79E-4	2.75
160	3.71E-5	2.91	3.71E-5	2.91	3.69E-5	2.91
320	4.67E-6	2.98	4.67E-6	2.98	9.03E-6	2.03
640	5.84E-7	3.00	5.84E-7	3.00	2.30E-6	1.97

L_∞ norm. Table 2 shows that the scheme preserves third order accuracy when parametrized limiters are applied with CFL being 1/5. It can also be observed from Table 1 & 2 that the accuracy of approximation degenerates to second order when large CFL number is used. We will not test the limiting procedure on other high order finite volume ENO, WENO schemes. However, those two examples indicate that the parametrized limiters applied to high order finite volume schemes do not compromise the order of accuracy of underlying schemes when the suitable CFL number is chosen.

3.3. **CFL constraint.** As revealed in the previous computation for both linear and nonlinear problems, the parametrized limiters guarantees the scheme to be MPP. Accuracy of the scheme will be decided by not only the order of the reconstructed polynomials, but also the CFL number because of the way CFL number being built into the limiters. We will devote this section to investigating how the CFL number affects the reconstruction of the high order numerical flux, thereby the overall accuracy of the numerical approximation to the exact solution. We will prove that the third order finite volume scheme with parametrized limiters preserves third order accuracy subject to mild CFL constraint. This is explained from the truncation error point of view. In the following analysis, we use linear advection problem as example for simplicity. However the analysis can be carried over to nonlinear problem without major difficulty since the analysis only depends on Taylor expansion, which is just algebraically more tedious in the nonlinear case. Before presenting the main result, we will introduce a few lemmas in order to prove the main theorem. In the following analysis, $O(h^3)$ denotes a number that $|O(h^3)| \leq ch^3$, where c is grid independent positive constant.

Lemma 6. *For a function $u(x)$, assuming $|D^{(\alpha)}u| \leq C$ for $\alpha \leq 3$, where C is a positive constant, if $\lambda \leq \sqrt{1/12}$, then*

$$(3.7) \qquad \bar{u}_j - \lambda(u_{j+\frac{1}{2}} - u_{j-\frac{1}{2}}) \leq u_M + O(h^3),$$

where $h = x_{j+\frac{1}{2}} - x_{j-\frac{1}{2}}$, $\bar{u}_j = \frac{1}{h}\int_{x_{j-\frac{1}{2}}}^{x_{j+\frac{1}{2}}} u dx$, $u_{j\pm\frac{1}{2}} = u(x_{j\pm\frac{1}{2}})$ and $u_M = \max u(x)$.

Proof. First, let us consider the case that u reaches maximum at $x_M \in [x_{j-\frac{1}{2}}, x_{j+\frac{1}{2}}]$. The other cases will be discussed separately. The Taylor expansion about x_M can be written as

$$(3.8) \qquad u(x) = u_M + u'(x_M)(x - x_M) + \frac{u''(x_M)}{2}(x - x_M)^2 + O(h^3).$$

Therefore, we have

$$(3.9) \qquad u(x) = u_M + \frac{u''(x_M)}{2}(x - x_M)^2 + O(h^3)$$

since $u'(x_M) = 0$. Now substitute $x = x_{j\pm\frac{1}{2}}$ into (3.9) and simplify, we have

$$(3.10) \qquad u(x_{j+\frac{1}{2}}) - u(x_{j-\frac{1}{2}}) = u''(x_M)h(x_j - x_M) + O(h^3).$$

Integrate (3.9) over $[x_{j-\frac{1}{2}}, x_{j+\frac{1}{2}}]$ to find $\bar{u}_j$ that

$$(3.11) \quad \bar{u}_j = u_M + \frac{u''(x_M)}{6h}\{(x_{j+\frac{1}{2}} - x_M)^3 - (x_{j-\frac{1}{2}} - x_M)^3\} + O(h^3).$$

Combine (3.10) with (3.11) and simplify, we have

$$(3.12) \qquad \bar{u}_j - \lambda(u_{j+\frac{1}{2}} - u_{j-\frac{1}{2}}) = u_M + u''(x_M)R + O(h^3),$$

where

$$(3.13) \qquad R(x_M) = \frac{1}{2}(x_M - x_j)^2 + h^2/24 - \lambda h(x_j - x_M).$$

To prove (3.7) from (3.12), **it suffices to show that $R \geq 0$ if $\lambda \leq \sqrt{1/12}$ since** $u''(x_M) \leq 0$. It is obvious $R(x_{j+\frac{1}{2}}) \geq 0$. In order for $R(x_{j-\frac{1}{2}}) \geq 0$, $\lambda \leq 1/3$ must hold. Differentiate R with respect to x_M, there is

$$(3.14) \qquad R'(x_M) = x_M - x_j + \lambda h.$$

R as function of x_M reaches its minimum at $x_c = x_j - \lambda h$

$$(3.15) \qquad R(x_c) = -\frac{1}{2}\lambda^2 h^2 + h^2/24.$$

We have $R(x_c) \geq 0$ when $\lambda \leq \sqrt{1/12}$.

If $u(x)$ reaches local maximum at $x_{j+\frac{1}{2}}$ or inside the interval $[x_{j-\frac{1}{2}}, x_{j+\frac{1}{2}}]$, then (3.7) automatically holds based on the above analysis. If $u(x)$ reaches its local maximum at $x_{j-\frac{1}{2}}$, then the Taylor expansion about $x_{j-\frac{1}{2}}$ takes the form

$$u(x) = u_{j-\frac{1}{2}} + u'(x_{j-\frac{1}{2}})(x - x_{j-\frac{1}{2}}) + \frac{u''(x_{j-\frac{1}{2}})}{2}(x - x_{j-\frac{1}{2}})^2 + O(h^3).$$

Following the previous calculation, we have

$$\bar{u}_j - \lambda(u_{j+\frac{1}{2}} - u_{j-\frac{1}{2}}) = u_{j-\frac{1}{2}} + u'(x_{j-\frac{1}{2}})(1/2 - \lambda)h$$

$$(3.16) \qquad\qquad\qquad + \frac{u''(x_{j-\frac{1}{2}})}{2}(1/3 - \lambda)h^2 + O(h^3).$$

When $\lambda \le 1/3$, (3.16) can be rewritten as

$$
\begin{aligned}
\bar{u}_j \quad - \quad & \lambda(u_{j+\frac{1}{2}} - u_{j-\frac{1}{2}}) \\
= \quad & u(x_{j-\frac{1}{2}} - h\sqrt{1/3 - \lambda}) + u'(x_{j-\frac{1}{2}})h(1/2 - \lambda + \sqrt{1/3 - \lambda}) + O(h^3)
\end{aligned}
$$

$$
(3.17) \quad \le \quad u_M + O(h^3)
$$

since $u'(x_{j-\frac{1}{2}}) \le 0$. Combining the above discussion, the lemma is proven.   □

Lemma 7. *If $\lambda \le 1/3$, then*

$$
(3.18) \qquad\qquad \bar{u}_j - \lambda(u_{j+\frac{1}{2}} - \bar{u}_{j-1}) \le u_M + O(h^3),
$$

where $\bar{u}_{j-1} = \frac{1}{h} \int_{x_{j-\frac{3}{2}}}^{x_{j-\frac{1}{2}}} u\,dx$.

Proof. Here we only consider the case that u reaches its maximum u_M inside the interval, the case that the accuracy is most likely to be affected by the limiters. Other cases can be considered like in Lemma 6. Again, use the Taylor expansion (3.9) to evaluate $u_{j+\frac{1}{2}}, \bar{u}_{j-1}$, we can have

$$
(3.19) \qquad\qquad \bar{u}_j - \lambda(u_{j+\frac{1}{2}} - \bar{u}_{j-1}) = u_M + u''(x_M)R + O(h^3),
$$

where

$$
\begin{aligned}
R(x_M) = \quad & \frac{1}{6h} \quad \{(x_{j+\frac{1}{2}} - x_M)^3 - (x_{j-\frac{1}{2}} - x_M)^3\} - \frac{\lambda}{2}(x_{j+\frac{1}{2}} - x_M)^2 \\
(3.20) \qquad & + \quad \frac{\lambda}{6h}\{(x_{j-\frac{1}{2}} - x_M)^3 - (x_{j-3/2} - x_M)^3\}.
\end{aligned}
$$

Once again, we have $R(x_{j+\frac{1}{2}}) > 0$ and $R(x_{j-\frac{1}{2}}) \ge 0$ when $\lambda \le 1/3$. It suffices to require $R(x_c) \ge 0$ at its critical points. Differentiate the form (3.20),

$$
(3.21) \qquad R'(x_M) = x_M - x_j - \lambda(x_M - x_{j+\frac{1}{2}}) + \lambda(x_M - \bar{x}_{j-1}),
$$

to find the critical point $x_c = x_j - \frac{3h}{2}\lambda$. The value of $R(x_c)$ is

$$
(3.22) \qquad\qquad R(x_c) = \frac{h^2}{4}(1/6 + 5/3\lambda - 9/2\lambda^2).
$$

This proves (3.18) since λ can be roughly computed as about 0.45 for $R \ge 0$.   □

To cover all the cases in the decoupling process, we also need

Lemma 8. *If $\lambda \le 1$, then*

$$
(3.23) \qquad\qquad \bar{u}_j - \lambda(\bar{u}_j - u_{j-\frac{1}{2}}) \le u_M + O(h^3).
$$

The is trivial due to the fact that the left side of (3.23) can be written as $(1 - \lambda)\bar{u}_j + \lambda u_{j-\frac{1}{2}} \le u_M$. With the help of Lemma 6, 7, 8, we can prove the main result.

Theorem 9. *For the third order finite volume reconstruction of numerical flux $\hat{H}_{j+\frac{1}{2}} = u^-_{j+\frac{1}{2}}$ to the advection equation, the redefined numerical flux $\tilde{H}_{j+\frac{1}{2}}$ by (2.5) maintains third order accurate approximation to $u_{j+\frac{1}{2}}$ when $CFL < \sqrt{1/12}$.*

Proof. Consider the limiters for the maximum value case. No limiters are introduced in case 1 decoupling, therefore accuracy is not affected. Starting with case 4, we would like to show that $\tilde{H}_{j+\frac{1}{2}}$ defined by (2.3) is third-order approximation

of $u_{j+\frac{1}{2}}$ if $\hat{H}_{j+\frac{1}{2}}$ is the third order approximation of $u_{j+\frac{1}{2}}$. It is sufficient to show that when $(\Lambda_{-\frac{1}{2},I_j}, \Lambda_{+\frac{1}{2},I_j}) = (\frac{\Gamma_j^M}{\lambda F_{j-\frac{1}{2}} - \lambda F_{j+\frac{1}{2}}}, \frac{\Gamma_j^M}{\lambda F_{j-\frac{1}{2}} - \lambda F_{j+\frac{1}{2}}})$ is chosen,

$$\Lambda_{+\frac{1}{2},I_j}(\hat{H}_{j+\frac{1}{2}} - \bar{u}_j) + \bar{u}_j - \hat{H}_{j+\frac{1}{2}} = O(h^3)$$

and

$$\Lambda_{-\frac{1}{2},I_j}(\hat{H}_{j-\frac{1}{2}} - \bar{u}_{j-1}) + \bar{u}_{j-1} - \hat{H}_{j-\frac{1}{2}} = O(h^3)$$

holds. We will prove the former estimate and the later is similar. This is equivalent to prove

$$(3.24) \qquad \frac{\Gamma_j - (\lambda F_{j-\frac{1}{2}} - \lambda F_{j+\frac{1}{2}})}{\lambda F_{j-\frac{1}{2}} - \lambda F_{j+\frac{1}{2}}} F_{j+\frac{1}{2}} = O(h^3),$$

when $\Gamma_j < \lambda F_{j-\frac{1}{2}} - \lambda F_{j+\frac{1}{2}}$. Since $F_{j-\frac{1}{2}} > 0$ and $F_{j+\frac{1}{2}} < 0$, $0 < -\frac{F_{j+\frac{1}{2}}}{\lambda F_{j-\frac{1}{2}} - \lambda F_{j+\frac{1}{2}}} \leq 1/\lambda$, recalling that

$$(3.25) \quad \Gamma_j - (\lambda F_{j-\frac{1}{2}} - \lambda F_{j+\frac{1}{2}}) = u_M - \{\bar{u}_j - \lambda(\hat{H}_{j+\frac{1}{2}} - \hat{H}_{j-\frac{1}{2}})\} < 0,$$

it suffices to show that

$$(3.26) \qquad u_M - \{\bar{u}_j - \lambda(\hat{H}_{j+\frac{1}{2}} - \hat{H}_{j-\frac{1}{2}})\} = O(h^3).$$

According to Lemma 6 and (3.7), we have $u_M - \{\bar{u}_j - \lambda(u_{j+\frac{1}{2}} - u_{j-\frac{1}{2}})\} \geq O(h^3)$. With $\hat{H}_{j\pm\frac{1}{2}} - u_{j\pm\frac{1}{2}} = O(h^3)$ and (3.25), it follows that

$$(3.27) \qquad O(h^3) \leq u_M - \{\bar{u}_j - \lambda(\hat{H}_{j+\frac{1}{2}} - \hat{H}_{j-\frac{1}{2}})\} < 0,$$

which means that (3.26) holds. For the case 2, we only need to consider when $\Lambda_{+\frac{1}{2},I_j} = \frac{\Gamma_j}{-\lambda F_{j+\frac{1}{2}}} < 1$ is chosen,

$$(3.28) \quad \tilde{H}_{j+\frac{1}{2}} - \hat{H}_{j+\frac{1}{2}} = \frac{\Gamma_j + \lambda F_{j+\frac{1}{2}}}{-\lambda} = \frac{u_M - \{\bar{u}_j - \lambda(\hat{H}_{j+\frac{1}{2}} - \bar{u}_{j-1})\}}{-\lambda}.$$

In order for $\tilde{H}_{j+\frac{1}{2}} - \hat{H}_{j+\frac{1}{2}} = O(h^3)$, it suffices to require $u_M - \{\bar{u}_j - \lambda(\hat{H}_{j+\frac{1}{2}} - \bar{u}_{j-1})\} = O(h^3)$. Notice that $\frac{\Gamma_j}{-\lambda F_{j+\frac{1}{2}}} < 1$ means

$$(3.29) \qquad u_M - \{\bar{u}_j - \lambda(\hat{H}_{j+\frac{1}{2}} - \bar{u}_{j-1})\} < 0.$$

However, from Lemma 7 and (3.18), we have

$$O(h^3) \leq u_M - \{\bar{u}_j - \lambda(u_{j+\frac{1}{2}} - \bar{u}_{j-1})\}.$$

Again, since $\hat{H}_{j+\frac{1}{2}} - u_{j+\frac{1}{2}} = O(h^3)$, it follows that

$$(3.30) \qquad O(h^3) \leq u_M - \{\bar{u}_j - \lambda(\hat{H}_{j+\frac{1}{2}} - \bar{u}_{j-1})\} < 0,$$

therefore, $u_M - \{\bar{u}_j - \lambda(\hat{H}_{j+\frac{1}{2}} - \bar{u}_{j-1})\} = O(h^3)$. We can conclude that the third order accuracy is maintained too in case 2. The case 3 is very similar to case 2. We shall not repeat it. □

To summarize, the third order finite volume scheme with parametrized limiters produce third order approximation of the numerical flux from the truncation point of view. The proof of Theorem 9 shows that we can have a general conclusion for polynomial reconstruction of order r that

Theorem 10. *If there exists a positive constant λ such that*

(3.31) $$\bar{u}_j - \lambda(u_{j+\frac{1}{2}} - u_{j-\frac{1}{2}}) \leq u_M + O(h^{r+1}),$$

(3.32) $$\bar{u}_j - \lambda(u_{j+\frac{1}{2}} - \bar{u}_{j-1})) \leq u_M + O(h^{r+1}),$$

(3.33) $$\bar{u}_j - \lambda(\bar{u}_j - u_{j-\frac{1}{2}}) \leq u_M + O(h^{r+1}),$$

then the newly defined flux $\tilde{H}_{j+\frac{1}{2}}$ is still $r + 1$-th order approximation of $u(x_{j+\frac{1}{2}})$, i.e., $\tilde{H}_{j+\frac{1}{2}} - u(x_{j+\frac{1}{2}}) = O(h^{r+1})$.

Therefore to extend this approach to higher order (higher than third order), it is equivalent to find suitable λ such that higher order version of Lemma 6, 7, 8 holds. In the next section, we will discuss how to establish a fourth order version of Lemma 6 as an example to extend the result and analysis to higher order. It is necessary to point out that even though the analysis and numerical test validates the claim stated in the Theorem 9, in both the Table 1 and 2 the third order of convergence can only be achieved for CFL number up to about $1/5$, which is less than the CFL number $\sqrt{1/12}$ given in the Theorem 9. This gap can be explained by:

(1) Same as what have been done in [12] and for most of the high order methods, the above analysis is purely for spatial discretization from the perspective of the truncation error. Which means that without considering time evolution, the truncation error and order of convergence for spatial discretization is on the scale of $O(h^3)$ for CFL number up to $\sqrt{1/12}$.

(2) When the MPP limiters are added onto the numerical fluxes, the limiters serve as hard caps on the intermediate values for the RK type time integration. As is well understood, the RK type time integration depends on the cancellation between lower order approximates to achieve high order accuracy. The hard caps introduced by the flux limiters inevitably create obstacles for the cancellation of low order terms, as has been observed in both [12] and this paper.

(3) The CFL number $\sqrt{1/12}$ is optimal estimate based on the results shown in Table 3.

To numerically verify those claims, for two functions, we compute the L_∞ measure of the spatial discretization error

$$(u(x_j + \frac{1}{2}h) - u(x_j - \frac{1}{2}h))/h - (\tilde{H}(x_j + \frac{1}{2}h) - \tilde{H}(x_j - \frac{1}{2}h))/h.$$

We compare the errors for different CFL numbers: CFL $= \sqrt{1/12}$ and slightly larger CFL $= 1.1 \times \sqrt{1/12}$ respectively. The results in Table 3 clearly indicate that third order accuracy is preserved for CFL number $\sqrt{1/12}$, while the spatial approximation degenerates for CFL number $1.1 \times \sqrt{1/12}$. For all the other μ we tried, the spatial discretization is uniform third order for CFL $= \sqrt{1/12}$.

3.4. **Fourth order finite volume scheme with parametrized limiters.**
In the previous section, for the third order finite volume scheme with the parametrized limiters it is proven that the limiters do not compromise the high order approximation of the flux. To illustrate the limiters can be applied to higher order, fourth order as example, we will give a lemma which is similar to Lemma 6 since Lemma

TABLE 3. Error and order of convergence for third order finite volume spatial approximation with parametrized MPP flux limiters: $u(x) = \sin(2\pi(x+\mu))$; Group 1: μ=0.39; CFL $= \sqrt{1/12}$; Group 2: $\mu = 0.39$; CFL $= 1.1 \times \sqrt{1/12}$; Group 3: $\mu = 0.58$; CFL $= \sqrt{1/12}$; Group 4: $\mu = 0.58$; CFL $= 1.1 \times \sqrt{1/12}$.

N	40	80	160	320	640	1280
Group 1	2.02E-3	2.53E-4	3.17E-5	3.96E-6	4.95E-7	6.19E-8
order		2.99	2.99	2.99	2.99	2.99
Group 2	4.35E-3	2.29E-3	1.16E-3	5.85E-4	2.91E-4	1.46E-4
order		0.92	0.98	0.99	0.99	0.99
Group 3	2.02E-3	2.53E-4	3.17E-5	3.96E-6	4.95E-7	6.19E-8
order		2.99	2.99	2.99	2.99	2.99
Group 4	1.42E-2	7.24E-3	3.63E-3	1.82E-3	9.10E-4	4.55E-4
order		0.97	0.99	0.99	0.99	0.99

(6, 7, 8) are essentially the sufficient conditions for the scheme to maintain high order accuracy.

Lemma 11. *For a function $u(x)$, assuming $|D^{(\alpha)}u| \leq C$ for $\alpha \leq 4$, if $\lambda < \sqrt{1/12}$, then*

$$(3.34) \qquad \bar{u}_j - \lambda(u_{j+\frac{1}{2}} - u_{j-\frac{1}{2}}) \leq u_M + O(h^4)$$

where the notation carries the same meaning as in Lemma 6.

Proof. First, we consider the case that u reaches maximum at $x_M \in [x_{j-\frac{1}{2}}, x_{j+\frac{1}{2}}]$. The Taylor expansion about x_M can be written as

$$
\begin{aligned}
u(x) \;=\; & u_M + u'(x_M)(x - x_M) + \frac{u''(x_M)}{2}(x - x_M)^2 \\
& + \frac{u'''(x_M)}{6}(x - x_M)^3 + O(h^4).
\end{aligned}
$$
(3.35)

Similar to the calculation for Lemma 6, after simplifying, we have the following

$$(3.36) \quad \bar{u}_j - \lambda(u_{j+\frac{1}{2}} - u_{j-\frac{1}{2}}) = u_M + \frac{u''(x_M)}{2}R_1 + \frac{u'''(x_M)}{6}R_2 + O(h^4),$$

where

$$(3.37) \qquad R_1(x_M) = (x_M - x_j)^2 + h^2/12 - 2\lambda h(x_j - x_M)$$

and

$$R_2(x_M) = \frac{1}{4h}\{(x_{j+\frac{1}{2}} - x_M)^4 - (x_{j-\frac{1}{2}} - x_M)^4\} - \lambda\{3h(x_M - x_j)^2 + \frac{h^3}{4}\}.$$

We seek a convex combination for (3.36) of the type

$$(3.38) \qquad L.H.S = \beta u(x_M + c_1 h) + (1 - \beta)u(x_M + c_2 h) + O(h^4),$$

where $0 \leq \beta \leq 1$, c_1, c_2 shall be bounded, i.e., $|c_1|, |c_2| < C_\lambda$ with $C_\lambda > 0$ and independent of h. To match (3.38) with (3.36) up to the $O(h^4)$ level truncation error after the Taylor expansion on the right hand of (3.38), we expect

$$(3.39) \qquad \beta c_1^2 + (1 - \beta)c_2^2 h^2 \leq R_1,$$
$$(3.40) \qquad \beta c_1^3 + (1 - \beta)c_2^3 h^3 = R_2,$$

which is a sufficient condition for the Lemma to hold since $u^{''}(x_M) \leq 0$. Let $c_1 = 0$, which means a combination with maximum point value, (3.39) can be simplified to one inequality

$$(3.41) \qquad\qquad (1 - \beta)R_2^2 \leq R_1^3.$$

Therefore $1 - \beta$ can be chosen as $min(1, \frac{R_1^3}{\max\limits_{x_M} R_2^2})$. Consequently, $c_2 = (\frac{R_2}{(1-\beta)h^3})^{1/3}$. When $\lambda < \sqrt{1/12}$, we have

$$(3.42) \qquad\qquad R_1 \geq \frac{h^2}{1/12 - \lambda^2}$$

by straightforward calculation (This is to obtain a lower bound on $1 - \beta$, therefore upper bound on $|c_2|$). Similar calculation for R_2 shows that

$$(3.43) \qquad\qquad \frac{\lambda h^3}{4} \leq \max_{x_{j-\frac{1}{2}} \leq x_M \leq x_{j+\frac{1}{2}}} |R_2| \leq \frac{(1 + 4\lambda)h^3}{4}.$$

(3.42) and (3.43) indicates there is a $c_0 > 0$ which only depends on λ such that $c_0 \leq 1 - \beta$ and $|c_2| \leq \frac{(1+4\lambda)}{4c_0}$. This means that β is well defined and c_2 is bounded in the sense there is $C_\lambda > 0$, dependent on λ only, such that $|c_2| \leq C_\lambda$. Since $u(x_M + c_2 h) \leq u_M$, the Lemma is proven in this case. For the other cases, we will not repeat the similar algebraic process. □

The above analysis indicates how the suitable CFL can be found for high order (higher than third order) schemes with parametrized limiters to maintain high order accuracy in terms of truncation error in spatial discretization. A less sharp CFL constraint can be obtained by using the Gauss Lobatto quadrature rules for $\bar{u}_j$ as used in [12]. However the Gauss Lobatto quadrature rule can not be applied to the analysis for the high order finite difference scheme with parametrized limiters. In the future, more efforts will be devoted to analyze the modified MPP flux limiters for high order scheme presented in Section 4. The modified flux limiters are designed in the similar way, but tailored for multiple stage time discretization. The successive flux limiting approach is more appealing since it allows significantly larger CFL number.

4. High order scheme with successively defined MPP flux limiters

In this section, we will discuss the implementation of the parametrized flux limiting technique to high order finite difference scheme. Through the numerical results, we would like to show that when the parametrized limiters are used to the third order finite difference scheme, both global maximum principle and third order accuracy are preserved. However, for the scheme to preserve third order accuracy in this framework, we experience a very restrictive CFL number constraint, namely $\frac{k}{h^{1.5}}\max\limits_{u}|f'(u)| \leq c$. It will be explained why the constraint is necessary through preliminary analysis. Most important of all, **a successively defined flux-limiters** strategy will be provided to relieve the very restrictive CFL constraint. The capability of this modified flux limiting technique shall be demonstrated through numerical experiments.

TABLE 4. Third order finite difference ENO scheme with parametrized limiters: Advection equation.

N	$\frac{k\alpha}{h^{1.5}}=1$		$\frac{k\alpha}{h}=0.1$		$\frac{k\alpha}{h}=0.25$	
	L_∞ error	order	L_∞ error	order	L_∞ error	order
40	2.16-3		2.15E-3		2.27-3	
80	2.72E-4	2.98	2.94E-4	3.00	4.07E-4	2.48
160	3.39E-5	3.00	3.49E-5	2.94	9.80E-5	2.05
320	4.22E-6	3.00	5.15E-6	2.76	2.47E-5	1.98
640	5.17E-7	3.00	9.97E-7	2.36	6.17E-6	2.00

4.1. Third order finite difference approximation with MPP property.
Consider the advection equation $f(u) = u$ with initial condition $u(x, 0) = \sin(2\pi x)$ on the interval $[0, 1]$. Let T be 1 which is one period of evolution. The only difference from Section 3.1 is the initial value. The rest of the limiting process is completely the same. For repeatedly refined uniform partition of the computational interval, Table 4 shows the scheme produces third order accuracy when the third order finite difference ENO scheme is used with the parametrized flux limiters. However, in this case, MPP and third order accuracy is obtained with the $\frac{k}{h^{1.5}} = 1$ type CFL condition. When the CFL number is on the scale of $\frac{k}{h} = O(1)$, the scheme degenerates to second order accuracy in L_∞ norm.

For the Burgers' equation considered in Section 3, we choose the first order Lax-Friedrich flux as the one that the high order flux is limited toward. The high order flux $\hat{H}_{j+\frac{1}{2}}$ is constructed in the way that

$$(4.1) \qquad \hat{H}_{j+\frac{1}{2}} = LF_{j+\frac{1}{2}}^- + LF_{j+\frac{1}{2}}^+.$$

$LF_{j+\frac{1}{2}}^-$ is reconstructed on the fixed stencil $S_j = \{I_{j-1}, I_j, I_{j+1}\}$ that

$$(4.2) \qquad LF_{j+\frac{1}{2}}^- = p(x_{j+\frac{1}{2}}), \frac{1}{h} \int_{I_l} p(x)dx = 1/2(f(u_l) + \alpha u_l), I_l \in S_j,$$

while $LF_{j-\frac{1}{2}}^+$ is reconstructed on the fixed stencil S_j that

$$(4.3) \qquad LF_{j-\frac{1}{2}}^+ = p(x_{j-\frac{1}{2}}), \frac{1}{h} \int_{I_l} p(x)dx = 1/2(f(u_l) - \alpha u_l), I_l \in S_j.$$

Again, $\alpha = \max_u |f'(u)|$, $p(x)$ is the polynomial of order 2. The result in Table 5 shows that the third order reconstruction with parametrized limiters applied to the Lax-Friedrich flux produces third order accurate approximation with very restrictive CFL number.

4.2. The CFL constraint.
The previous computation shows that the third order finite difference scheme with parametrized limiters is MPP while maintaining third order accuracy for both linear and nonlinear problem. However, there is a stiff CFL constraint for the scheme to function properly. We would like to explain why it is necessary using linear advection as example. Following the previous analysis, in order for the scheme to preserve maximum principle and maintain high order accuracy, it seems the lemma of the following type holds the key.

TABLE 5. Third order finite difference scheme with parametrized limiters: Burgers' equation.

N	$\frac{k\alpha}{h^{1.5}}=1$		$\frac{k\alpha}{h}=0.2$		$\frac{k\alpha}{h}=0.4$	
	L_∞ error	order	L_∞ error	order	L_∞ error	order
40	2.43E-3		2.43E-3		2.43-3	
80	3.21E-4	2.92	3.21E-4	2.92	3.16E-4	2.93
160	3.98E-5	3.01	3.98E-5	3.01	5.05E-5	2.64
320	4.84E-6	3.04	4.83E-6	3.04	1.33E-5	1.91
640	5.94E-7	3.02	9.22E-7	2.39	3.41E-6	1.96

Lemma 12. *If* $\lambda = ch^{0.5}$, *where c is a positive constant, then*

$$(4.4) \qquad u_j - \lambda(H_{j+\frac{1}{2}} - H_{j-\frac{1}{2}}) \le u_M + O(h^3),$$

where H is defined by $u(x) = \frac{1}{h}\int_{x-h/2}^{x+h/2} H dx$ *as in* [9].

Proof. : Assuming u obtains maximum on the interval $[x_{j-\frac{1}{2}}, x_{j+\frac{1}{2}}]$, it follows the Taylor expansion that

$$(4.5) \qquad u(x) = u_M + \frac{u''(x_M)}{2}(x - x_M)^2 + O(h^3).$$

By the definition of H, we have

$$(4.6) \qquad H(x) = u_M + \frac{u''(x_M)}{2}\{(x - x_M)^2 - h^2/12\} + O(h^3).$$

Therefore, by substitution and simplification, it follows that

$$(4.7) \qquad u_j - \lambda(H_{j+\frac{1}{2}} - H_{j-\frac{1}{2}}) = u_M + u''(x_M)R + O(h^3),$$

where $R = \frac{1}{2}(x_j - x_M)^2 + \lambda h(x_M - x_j)$. In order to satisfy (4.4), it suffices to require that $R \ge 0$ or $R = O(h^3)$. Since $R(x_M)$ has minimum value $-\frac{1}{2}\lambda^2 h^2$ at its critical point $x_c = x_j - \lambda h$, it is necessary to require that $\lambda^2 h^2 \le ch^3$ in order for (4.4) to hold. Thereby, $\lambda \le ch^{0.5}$. $\square$

The purpose of this preliminary analysis is to point out that the stiff constraint on the CFL number comes from the requirement that each intermediate value in the RK steps should lie within the range of the initial value. In the next section, we will tailor the parametrized flux limiting approach for multi-stage TVD RK time stepping to adopt large CFL number without compromising the overall accuracy of the underlying high order schemes while preserving the strict maximum principle.

4.3. **Successive parametrized limiters in multi-stage TVD RK method: The main algorithm.** In this section, we will present the main algorithm with the flux limiting technique discussed in Section 2 as the building block. The main algorithm is designed by combining the limiting process with relaxed bounds for the TVD RK time discretization.

Since the intermediate value of the multi-stage RK methods carries no valuable meaning to the final numerical solution except that its combination produces high order accurate approximation, it is reasonable not to enforce intermediate value into the range $[u_m, u_M]$. Therefore, the stiff constraint on the CFL number can be

relaxed. To demonstrate this idea, we use the third order RK method (3.1) for the problem (1.3) as an example to give full description of this new approach.

Remember what is really expected is $u_m \leq u_j^{n+1} \leq u_M$. Formulation wise, this means that the third step in (3.1) can be enforced in the manner that

$$(4.8) \qquad u_m \leq \frac{1}{3} u_j^n + \frac{2}{3}(u_j^{(2)} + \Delta t L(u^{(2)})) \leq u_M.$$

Therefore for the embedded Euler forward step in (4.8), this is equivalent to

$$(4.9) \qquad \frac{3}{2} u_m - \frac{1}{2} u_j^n \leq u_j^{(2)} + \Delta t L(u^{(2)}) \leq \frac{3}{2} u_M - \frac{1}{2} u_j^n.$$

To achieve this in the previously described parametrized limiting process for the one step Euler forward method, a sufficient requirement for $u_j^{(2)}$ in the conservative form (2.1) (limiting the high order flux toward the first order upwinding flux) shall be

$$(4.10) \quad \Phi_j = \max(\phi_{j-1}, \phi_j, \phi_{j+1}) \leq u_j^{(2)} \leq \Psi_j = \min(\psi_{j-1}, \psi_j, \psi_{j+1}),$$

where $\Phi_j = \frac{3}{2} u_m - \frac{1}{2} u_j^n$ and $\Psi_j = \frac{3}{2} u_M - \frac{1}{2} u_j^n$. The upper and lower bounds enforced in (4.10) are much less demanding than the requirement $u_m \leq u_j^{(2)} \leq u_M$ since $\phi_j \leq u_m$ and $\psi_j \geq u_M$. Consequently, the Euler forward in the second stage of the RK method can also be relaxed to the following form

$$(4.11) \qquad \Phi_j \leq \frac{3}{4} u_j^n + \frac{1}{4}(u_j^{(1)} + \Delta t L(u^{(1)})) \leq \Psi_j.$$

In the one step Euler forward formulation, this is

$$(4.12) \qquad \xi_j = 4\Phi_j - 3u_j^n \leq u_j^{(1)} + \Delta t L(u^{(1)}) \leq \eta_j = 4\Psi_j - 3u_j^n.$$

Again, to achieve this in the parametrized limiters approach for the one step Euler forward method, a sufficient requirement for $u_j^{(1)}$ shall be

$$(4.13) \qquad \Xi_j = \max(\xi_{j-1}, \xi_j, \xi_{j+1}) \leq u_j^{(1)} \leq \Omega_j = \min(\eta_{j-1}, \eta_j, \eta_{j+1}),$$

which simply means for the first step in the RK steps, we will only need

$$(4.14) \qquad \Xi_j \leq u_j^n + \Delta t L(u^n) \leq \Omega_j$$

instead of the previous stiff requirement $u_m \leq u_j^n + \Delta t L(u^n) \leq u_M$. (4.10) and (4.13) are sufficient conditions for the first order monotone scheme to satisfy the bounds in (4.9) and (4.12). Therefore they ensure the existence of meaningful limiters. To fully implement the above modified constraint in the parametrized limiters approach, basically, it only requires to redefine Γ_j^M and Γ_j^m. For the third order RK method, in the maximum value case, at the first stage Γ_j^M can be redefined by

$$(4.15) \qquad \Gamma_j^M = \Omega_j - u_j^n + \lambda(\hat{h}_{j+\frac{1}{2}}^n - \hat{h}_{j-\frac{1}{2}}^n) \geq 0,$$

while at the second stage

$$(4.16) \qquad \Gamma_j^M = \eta_j - u_j^{(1)} + \lambda(\hat{h}_{j+\frac{1}{2}}^{(1)} - \hat{h}_{j-\frac{1}{2}}^{(1)}) \geq 0,$$

and at the final stage

$$(4.17) \qquad \Gamma_j^M = \psi_j - u_j^{(2)} + \lambda(\hat{h}_{j+\frac{1}{2}}^{(2)} - \hat{h}_{j-\frac{1}{2}}^{(2)}) \geq 0.$$

In the minimum value case, for the three steps, Γ_j can be redefined by

$$(4.18) \qquad \Gamma_j^m = \Xi_j - u_j^n + \lambda(\hat{h}_{j+\frac{1}{2}}^n - \hat{h}_{j-\frac{1}{2}}^n) \leq 0,$$

in the first step

$$(4.19) \qquad \Gamma_j^m = \xi_j - u_j^{(1)} + \lambda(\hat{h}_{j+\frac{1}{2}}^{(1)} - \hat{h}_{j-\frac{1}{2}}^{(1)}) \leq 0,$$

in the second step and

$$(4.20) \qquad \Gamma_j^m = \phi_j - u_j^{(2)} + \lambda(\hat{h}_{j+\frac{1}{2}}^{(2)} - \hat{h}_{j-\frac{1}{2}}^{(2)}) \leq 0$$

in the final step. With those redefined steps, we would like to make the following comments.

Remark 13. *The modified limiters bounds updated values differently cell by cell and step by step. This is very different from the limiters given in Section 2, where universal bounds are set as u_m, u_M.*

Remark 14. *To ensure existence of parametrized limiters such that (4.9), (4.12) and (4.14) holds, therefore (4.8) to be true, we only need the inequalities in (4.15)—(4.20) to be true when updating with first order upwinding scheme. This can be checked consecutively from step 1 to step 3 using the definition of those limits for each of the steps.*

Since the algorithm presented above assumes that the first order numerical flux includes two point values, the successive bounds shall be modified if the first order monotone flux includes more than two point values. For the intermediate stages, the truncation error is no longer at the level of designed accuracy. Therefore it is unclear to the author how a thorough analysis of the scheme shall be laid out at this moment. For other explicit time integration strategy, the corresponding limiters can be designed in the similar way. The high order scheme with modified limiters preserves strict maximum principle. The remaining question is whether it maintains high order accuracy. In the next section, we will demonstrate that high order accuracy is not compromised even when significantly large CFL number is used.

4.4. CFL constraint revisited: Numerical tests. In this section, we would like to demonstrate the capability of the successively defined flux limiting technique for the multi-stage RK time stepping.

Test 1: Third order finite difference and finite volume scheme with successive MPP flux limiters. The linear and nonlinear problems tested in previous sections will be recomputed by applying the successively defined parametrized limiters to the third order finite volume (FV) and finite difference (FD) scheme. CFL number is chosen to be 0.6 for finite volume computation and 0.3 for finite difference. The results in Table 6 show that with the modified flux limiters, third order convergence (measured in L_∞ norm) is achieved for all four cases. When applied to the high order finite difference scheme, full analysis of the order of convergence is very difficult if not impossible at this moment even from truncation point of view. The reason is that the intermediate values are not high order approximation to any meaningful analytic values. The full analysis of order of convergence also involves order of accuracy in time discretization, which is not the main topic in this paper. Nonetheless, the technique can be generalized to schemes of any order.

TABLE 6. Error and order of convergence for third order finite volume and finite difference scheme with successively defined limiters.

	FV; Advection		FV; Burgers		FD; Advection		FD; Burgers	
N	error	order	error	order	error	order	error	order
40	2.33E-3		1.86E-3		2.20E-3		2.43E-3	
80	2.94E-4	2.98	2.76E-4	2.75	2.74E-4	3.00	3.19E-4	2.98
160	3.66E-5	3.00	3.65E-5	2.91	3.41E-5	3.00	3.97E-5	3.00
320	4.55E-6	3.00	4.60E-6	2.98	4.23E-6	3.01	4.83E-6	3.04
640	5.66E-7	3.00	5.75E-7	3.00	5.24E-7	3.01	5.93E-7	3.02

The difficulty is also related to the fact that we are applying different bounds for each of the intermediate steps in a multi-stage TVD RK time integration. Those different bounds further complicate the analysis of the time discretization accuracy due to reasons stated in Section 3.3.

To make up for the lack of thorough analysis of the order of convergence for high order schemes with parametrized limiters, we will provide more numerical tests to demonstrate the capability of this approach. For the linear advection problem, we choose $u_0(x) = \sin(2\pi x)^4$ as initial condition for finite volume and $u_0(x) = \sin(2\pi x)^6$ for finite difference with fixed stencil to reconstruct the high order numerical flux. L_∞ errors are computed for refined grids and results are compared with that without parametrized limiters. The CFL number again is chosen to be 0.6 for finite volume and 0.3 for finite difference scheme. We run the simulation to $T = 1$. The difference of this example with the previous one is that the solution in this case has a relatively large flat valley where the numerical value most likely exceeds its original bounds and the limiters are frequently triggered. The example for finite difference test is tougher because of the square profile of the initial value. Therefore, we hope that those two examples will help validate this new approach. The results in Table 7 and 8 indicate that for all the refined grids, the numerical solution exceeds the upper and lower bound of the initial value for fixed stencil reconstruction without limiters. However, when the parametrized limiters are applied, the numerical solution stays within the initial bounds up to the machine error. Third order convergence is observed in all the simulation.

TABLE 7. Error and order of convergence for third order finite volume scheme w/o successively defined limiters for advection equation; WO=without limiters, WL=with limiters; $u_0(x) = \sin(2\pi x)^4$.

N	40	80	160	320	640	1280
WO: error	6.90E-2	1.07E-2	1.39E-3	1.75E-4	2.19E-5	2.74E-6
order		2.67	2.95	2.99	2.99	2.99
$\min(u_h)$	-3.42E-2	-6.29E-3	-8.33E-4	-1.05E-4	-1.31E-5	-1.64E-6
WL: error	6.79E-2	1.07E-2	1.39E-3	1.98E-4	2.71E-5	3.46E-6
order		2.65	2.94	2.81	2.87	2.96
$\min(u_h)$	8.92E-25	5.63E-33	1.94E-30	3.80E-23	6.26E-26	3.48E-21

TABLE 8. Error and order of convergence for third order finite
difference scheme w/o successively defined limiters for advection
equation; WO=without limiters, WL=with limiters; $u_0(x) =$
$\sin(2\pi x)^6$.

N	40	80	160	320	640	1280
WO: error	1.16E-1	2.24E-2	3.04E-3	3.84E-4	4.81E-5	6.02E-6
order		2.37	2.88	2.98	2.99	2.99
$\min(u_h)$	-3.36E-2	-4.14E-3	-3.77E-4	-2.11E-5	-1.00E-6	-4.51E-8
WL: error	1.14E-1	2.24E-2	3.04E-3	3.84E-4	4.81E-5	6.02E-6
order		2.34	2.88	2.98	2.99	2.99
$\min(u_h)$	7.77E-22	4.72E-57	3.73E-36	4.33E-38	4.97E-40	3.17E-37

**Test 2: Fifth order finite difference and finite volume WENO scheme
with successive MPP flux limiters.** We also test the successive flux limiting
technique to fifth order finite volume and finite difference WENO schemes for the
advection equation and the Burgers' equation. For the advection problem, we
choose initial value as $u_0(x) = sin(2\pi x)^4$ on the interval $[0, 1]$ assuming periodic
boundary condition. We run the simulation to $T = 0.2$ with $k = 0.6h^{5/3}$ for both
finite volume and finite difference computation. The minimum numerical value, the
numerical errors measured in L_∞ norm and order of convergence are documented in
Table 9 for fifth order finite volume WENO scheme and Table 10 for finite difference
WENO scheme. The results indicate that the fifth order finite volume and finite
difference WENO scheme with successive MPP flux limiters produces fifth order
accurate numerical solution while preserving the strict maximum principle.

TABLE 9. Error and order of convergence for fifth order finite vol-
ume WENO scheme w/o successively defined limiters for advection
equation; WO=without limiters, WL=with limiters; $u_0(x) =$
$\sin(2\pi x)^4$.

N	20	40	80	160	320	640
WO: error	2.35E-2	1.00E-3	3.43E-5	1.06E-6	3.32E-8	1.04E-9
order		4.54	4.91	4.97	4.99	4.99
$\min(u_h)$	-1.79E-2	-7.60E-4	-2.18E-5	-4.59E-7	4.00E-10	9.40E-10
WL: error	2.40E-2	1.05E-3	5.41E-5	1.90E-6	6.45E-8	2.08E-9
order		4.51	4.28	4.82	4.88	4.95
$\min(u_h)$	1.62E-16	2.97E-14	3.22E-14	6.28E-8	1.30E-8	1.26E-9

We also compute the Burgers' equation with fifth order finite volume and finite
difference WENO scheme with the same setup as in **Test 1**. Table 11 and 12 shows
that both the finite volume and the finite difference fifth order WENO schemes
with the successive MPP flux limiters produce fifth order accurate solution.

To demonstrate that the fifth order scheme with successive MMP flux limiters
preserves strict maximum principle for nonlinear problems, we test the fifth order
finite difference scheme on the Burgers' equation with discontinuous initial condition

$$u_0(x) = \begin{cases} 0 & x \leq 0.5, \\ 1 & x > 0.5. \end{cases}$$

TABLE 10. Error and order of convergence for fifth order finite difference WENO scheme w/o successively defined limiters for advection equation; WO=without limiters, WL=with limiters; $u_0(x) = \sin(2\pi x)^4$.

N	20	40	80	160	320	640
WO: error	5.44E-2	5.29E-3	8.75E-4	2.99E-5	7.16E-7	1.14E-8
order		3.36	2.59	4.87	5.38	5.96
$\min(u_h)$	-9.54E-3	-1.28E-3	-2.27E-4	-8.14E-6	2.31E-8	-3.37E-10
WL: error	5.21E-2	4.77E-3	6.33E-4	2.89E-5	7.16E-7	1.14E-8
order		3.44	2.91	4.45	5.33	5.96
$\min(u_h)$	3.03E-3	4.23E-4	9.97E-6	3.01E-7	7.35E-10	2.46E-10

TABLE 11. Error and order of convergence for fifth order finite volume WENO scheme w/o successively defined limiters for Burgers' equation; WO=without limiters, WL=with limiters; $u_0(x) = 0.5(1 + \sin(2\pi x))$.

N	20	40	80	160	320	640
WO: error	4.49E-3	5.33E-4	2.65E-5	9.64E-7	3.09E-8	9.70E-10
order		3.07	4.32	4.78	4.95	4.99
$\min(u_h)$	7.78E-3	2.00E-3	5.05E-4	1.27E-4	3.19E-5	8.00E-6
WL: error	4.49E-3	5.33E-4	2.65E-5	9.64E-7	3.09E-8	9.70E-10
order		3.07	4.32	4.78	4.95	4.99
$\min(u_h)$	7.78E-3	2.00E-3	5.05E-4	1.27E-4	3.19E-5	8.00E-6

TABLE 12. Error and order of convergence for fifth order finite difference WENO scheme w/o successively defined limiters for Burgers' equation; WO=without limiters, WL=with limiters; $u_0(x) = 0.5(1 + \sin(2\pi x))$.

N	20	40	80	160	320	640
WO: error	1.05E-2	1.18E-3	5.92E-5	2.00E-6	6.19E-8	1.90E-9
order		3.15	4.32	4.88	5.01	5.01
$\min(u_h)$	6.92E-3	1.60E-3	3.90E-4	9.63E-5	2.39E-5	6.00E-6
WL: error	1.05E-2	1.18E-3	5.92E-5	2.00E-6	6.19E-8	1.90E-9
order		3.15	4.32	4.88	5.01	5.01
$\min(u_h)$	6.92E-3	1.60E-3	3.90E-4	9.63E-5	2.39E-5	6.00E-6

The results in Table 13 clearly indicate the maximum principle is preserved. We would like to summarize the results into a comment that

Remark 15. *Within the parametrized limiters framework provided in this paper, high order finite volume and finite difference scheme with successively defined MPP limiters for the multi-stage RK method allows for significantly large CFL number while preserving maximum principle and high order accuracy.*

TABLE 13. Fifth order finite difference WENO scheme w/o successively defined limiters for Burgers' equation; WO=without limiters, WL=with limiters.

N	20	40	80	160	320	640
WO: $\min(u_h)$	-5.62E-5	-2.93E-5	-7.09E-5	-7.76E-5	-1.12E-4	-1.03E-4
WL: $\min(u_h)$	5.73E-14	2.14E-15	1.13E-15	9.75E-22	1.64E-38	3.16E-72

5. CONCLUSION

In this paper, we proposed a novel approach to design high order maximum principle preserving schemes for hyperbolic conservation laws within the flux limiters framework. The parametrized limiters are derived from decoupling a sequence of explicit inequalities bounding the updated values. To the best knowledge of the author, this simple and straightforward decoupling technique is surprisingly first ever used to limiters for high order schemes. Different from the existing method in the literature, the new strategy does not demand the rescaling of the reconstructed polynomial around its average into a range of absolute reference values. This flexibility allows for a less restrictive CFL number. Within the parametrized limiters framework, both high order finite volume and finite difference schemes can be designed to preserve maximum principle and high order accuracy. Analysis and numerical evidence indicates that the high order finite difference scheme with parametrized limiters preserve strict maximum principle while maintaining high order accuracy with suitable CFL condition. The flexibility of the parametrized flux limiters also allows for a successive parametrized limiting process for multi-stage RK time discretization. The new successive limiting process adopts significantly large CFL number for both high order finite volume and finite difference MPP schemes. Complete analysis of the successively parametrized limiters for high order finite difference scheme will be part of the future work. The decoupling of the parameters in two-dimensional case will also be investigated. A systematic analysis of the relation between achieving high order accuracy and CFL number shall be explored in the future.

6. ACKNOWLEDGEMENT

REFERENCES

1. A. Harten, *High resolution schemes for conservation laws*, Journal of Computational Physics, 49 (1983), 357-393.
2. A. Harten, B. Engquist, S. Osher and S. R. Chakravarty, *Uniformly high order accurate essentially non-oscillatory schemes, III*, Journal of Computational Physics, 71 (1987) 231-303.
3. X.-D. Liu, S. Osher, *Non-oscillatory high order accurate self-similar maximum principle satisfying shock capturing schemes*, SIAM Journal on Numerical Analysis, 33 (1996) 760-779.
4. S. Osher, *Riemann solvers, the entropy condition and difference approximations*. SIAM Journal on Numerical Analysis, 21 (1984), 217-235.

5. S. Osher and S. Chakravarthy, *High resolution schemes and the entropy condition*, SIAM Journal on Numerical Analysis, 21 (1984), 955-984

6. A. M. Rogerson, E. Meiburg, *A numerical study of the convergence properties of ENO schemes*, Journal of Scientific Computing, 5 (1990), 151-167.

7. R. Sanders, *A third-order accurate variation nonexpansive difference scheme for single nonlinear conservation law*, Mathematics of Computation, 51 (1988), 535-558.

8. C.-W. Shu, S. Osher, *Efficient implementation of essentially non-oscillatory shock-capturing schemes*, Journal of Computational Physics, 77 (1988), 439-471.

9. C.-W. Shu, S. Osher, *Efficient implementation of essentially non-oscillatory shock-capturing schemes, II*, Journal of Computational Physics, 83 (1989), 32-78.

10. P. K. Sweby, *High resolution schemes using flux limiters for hyperbolic conservation laws*, SIAM Journal on Numerical Analysis, 21 (1984), 995-1011.

11. Z. Xu, C.-W. Shu, *Anti-diffusive flux corrections for high order finite difference WENO schemes*, Journal of Computational Physics, 205 (2005), 458-485.

12. X. Zhang and C.-W. Shu, *On maximum-principle-satisfying high order schemes for scalar conservation laws*, Journal of Computational Physics, 229 (2010), 3091-3120.

13. X. Zhang and C.-W. Shu, *On positivity preserving high order discontinuous Galerkin schemes for compressible Euler equations on rectangular meshes*, Journal of Computational Physics, 229 (2010), 8918-8934.

14. X. Zhang and C.-W. Shu, *A genuinely high order total variation diminishing scheme for one-dimensional scalar conservation laws*, SIAM Journal on Numerical Analysis, 48 (2010), 772-795.

15. X. Zhang and C.-W. Shu, *Positivity-preserving high order finite difference WENO schemes for compressible Euler equations*, Journal of Computational Physics, 231 (2012), 2245-2258.

DEPARTMENT OF MATHEMATICAL SCIENCE, MICHIGAN TECH UNIVERSITY, HOUGHTON, MI 49931
E-mail address: `zhengfux@mtu.edu`